Control-limited perfect state transfer, quantum stochastic resonance and many-body entangling gate in imperfect qubit registers

C. Di Franco[1], M. Paternostro[1], D. I. Tsomokos[2], and S. F. Huelga[2]
[1] *School of Mathematics and Physics, Queen's University, Belfast BT7 1NN, United Kingdom*
[2] *Quantum Physics Group, STRI, School of Physics, Astronomy & Mathematics, University of Hertfordshire, Hatfield, AL10 9AB, United Kingdom*
(Dated: July 8, 2008)

We propose a protocol for perfect quantum state transfer that is resilient to a broad class of realistic experimental imperfections, including noise sources that could be modelled either as independent Markovian baths or as certain forms of spatially correlated environments. We highlight interesting connections between the fidelity of state transfer and quantum stochastic resonance effects. The scheme is flexible enough to act as an effective entangling gate for the generation of genuine multipartite entanglement in a control-limited setting. Possible experimental implementations using superconducting qubits are also briefly discussed.

PACS numbers: 03.67.-a, 75.10.Pq

I. INTRODUCTION

In the last few years, it has been realized that specific forms of built-in and permanent intra-register couplings could be used for the purposes of quantum computation and communication [1, 2]. These methods allow us to bypass the need for both fast and accurate inter-qubit switching and gating, which are generally very demanding tasks. We refer to such schemes – where the required external control over physical systems is greatly reduced – as *control-limited*. However, the price to pay for the performance of efficient operations is the need to pre-engineer appropriate patterns of couplings. Determining the exact distribution of coupling strengths for a given interaction model in a control-limited setting is often a matter of craftsmanship or the result of the exploitation of certain geometrical properties of the system at hand [3, 5]. A simple physical model suitable for this scenario is provided by a linear spin chain. Here we use the term "spin chain" in its wider sense which includes other physical systems as well that can be modelled by a generic spin chain Hamiltonian.

In the quest for the realization of a realistic quantum processor, the achievement of faithful transmission of quantum information has been the object of remarkable interest. The possibility of linking different local nodes of a quantum network through photons has been exhaustively analyzed [4]. For short-distance quantum communication, the idea of using spin chains as *quantum wires* has been put forward by Bose [5]. With an isotropic Heisenberg interaction a transmission fidelity that exceeds the maximum value achievable classically can be obtained for a chain of up to ~ 80 qubits. The original idea has then been extended along various directions [6]. In particular, Christandl *et al.* [3] showed that, by engineering the strength of the couplings in the chain, perfect state transfer could be achieved.

At the same time, quantum entanglement (bi-partite as well as multi-partite) has been studied in great detail over the last years [1, 7] and appears to be a key resource for many applications in quantum information processing (QIP). It is well-known that genuine multipartite entanglement of Greenberger-Horne-Zeilinger (GHZ) form [8] is useful for multi-agent protocols of distributed QIP such as quantum secret sharing, remote implementation of unknown operations, quantum average estimation and quantum anonymous transmission [9, 10]. Our study is thus distinguished, for instance, with respect to the investigation in [11], which was centered on cluster state generation in quantum spin chains.

Here we show how to make use of a physical system whose Hamiltonian can be mapped into that of a spin chain in order to achieve both these goals: With the same system we are able to transfer the state from one qubit to another or to generate GHZ entanglement. In addition to pragmatic goals relevant to quantum information processing, our study reveals an interesting non-monotonic behavior of state-transfer fidelity against the strength of the external noise. This reminds us of quantum stochastic resonances in many-body systems [12] and represents an original way of revealing these fundamentally interesting processes in a linear register of qubits. A possible physical implementation of the proposed system could be provided by a chain of superconducting qubits [13, 14, 15] in which each qubit operates at its degeneracy point [16]. One of the main reasons for this choice is related with the remarkable recent advances in experiments with coupled superconducting qubits [17, 18, 19]. The fabrication of chains of $N \sim 50$ Josephson qubits has been achieved in the laboratory and their coherent operation is a foreseeable possibility [20].

The remainder of the paper is organized as follows. In Sec. II we describe the system we use either to obtain a perfect state transfer or to generate multipartite entanglement of GHZ form. In Sec. III we explain in details these two protocols while in Sec. IV the effects of static disorder, decay and decoherence on these schemes are studied. Finally, in Sec. V we summarize our results.

II. THE SYSTEM AND THE INFORMATION-FLUX APPROACH

The system we analyze is an open spin-chain of N qubits, whose Hamiltonian reads

$$\hat{\mathcal{H}} = \sum_{i=1}^{N-1} J_i \hat{Z}_i \hat{Z}_{i+1} + \sum_{i=1}^{N} B_i \hat{X}_i, \tag{1}$$

where J_i is the coupling strength of the pairwise interaction between qubit i and $i+1$ and B_i is a local magnetic field on qubit i. In our notation, $\hat{X}$, $\hat{Y}$ and $\hat{Z}$ denote the x, y and z-Pauli matrix, respectively. The model in Eq. (1) describes, for instance, a chain of interacting superconducting qubits, each at its degeneracy point [13, 15, 16]. Here, in order to keep our discussion on the most general level, free from a specific setup, we interpret $\hat{\mathcal{H}}$ as a generic spin-chain model.

An important remark is due. Frequently one faces the case of dynamics ruled by spin-preserving Hamiltonian models (*i.e.* Hamiltonians that commute with the total spin operator of the system). By assuming appropriate boundary conditions, it is then convenient to diagonalize the coupling Hamiltonian by means of a sequence comprising Wigner-Jordan, Fourier, and Bogoliubov transformations [21]. In our case, $\hat{\mathcal{H}}$ does not preserve the total number of excited spins, so that the mutual coupling among subspaces labeled by different numbers of spin-excitation has to be considered. Rather than applying techniques for the exact solution of Eq. (1) [21], we propose to tackle the evolution of the system by means of an *information-flux approach* (IFA) which is specifically designed for multi-spin interactions [22]. Our method does not rely on the explicit analysis of the chain's spectrum and enables us to gather an intuitive picture of the dynamics at hand.

On a formal level, the IFA requires the time-evolved form of specific operators $\hat{\tilde{O}}_i$ in the Heisenberg picture, *i.e.* $\hat{\tilde{O}}_i(t) = e^{i\hat{\mathcal{H}}t}\hat{O}_i e^{-i\hat{\mathcal{H}}t}$ (here $O = X, Y, Z$ and $i = 1, .., N$). This allows one to understand the dependence of $\hat{\tilde{O}}_i$ on any $\hat{O}_j$ and to design the set of coupling strengths $\{J_i\}$ in such a way that it becomes possible to *drive* a desired evolution by means of engineered quantum interference [22]. Our task here is the transmission of quantum information from the first qubit to the last one in the chain. This requires the study of $\hat{\tilde{O}}_N(t)$'s, which can be decomposed into the operator-basis built out of all possible tensorial products of $\{\hat{X}_i, \hat{Y}_i, \hat{Z}_i\}$. Therefore, we can write $\langle\Psi_0|\hat{\tilde{O}}_N(t)|\Psi_0\rangle = \sum_{O'=X,Y,Z,I} \mathcal{I}^{OO'}(t)\langle\phi_0|\hat{O}'_1|\phi_0\rangle$, where $|\Psi_0\rangle = |\phi_0\rangle_1 \otimes |\psi_0\rangle_{2..N}$ is the initial state of the whole chain, $|\phi_0\rangle$ is the initial state of the first qubit only and $|\psi_0\rangle_{2..N}$ is the state of the rest of the chain. The coefficient $\mathcal{I}^{OO'}(t)$ is defined as the information flux at time t from $\hat{O}'_1$ to $\hat{O}_N$ [22]. It is easy to see that if our system achieves $|\mathcal{I}^{OO'}| = 1$ when $O = O'$, we have perfect $1 \to N$ state transfer.

To give an immediate picture of IFA, we discuss here a simple but yet helpful application of the method. We consider a three-qubit open chain whose Hamiltonian reads $\hat{\mathcal{H}}_E = J(\hat{X}_1\hat{X}_2 + \hat{Y}_1\hat{Y}_2 + \hat{X}_2\hat{X}_3 + \hat{Y}_2\hat{Y}_3)$. By solving the corresponding Schrödinger equation, it is well known that perfect state transfer from the first to the third qubit is achieved in this case when the initial state of second and third qubit is $|00\rangle_{23}$ and waiting a time $t = \pi/(2\sqrt{2}J)$ [3]. By analyzing the evolution of the operator $\hat{X}_3$, we find $\hat{\tilde{X}}_3(t) = -\sin^2(\sqrt{2}Jt)\hat{X}_1\hat{Z}_2\hat{Z}_3 - (1/\sqrt{2})\sin(2\sqrt{2}Jt)\hat{Y}_2\hat{Z}_3 + \cos^2(\sqrt{2}Jt)\hat{X}_3$. Similar results are obtained by looking at the evolution of $\hat{Y}_3$ and $\hat{Z}_3$. Therefore, the information flux from $\hat{X}_1$ to $\hat{X}_3$ is $\mathcal{I}^{XX} = -\sin^2(\sqrt{2}Jt)_{2,3}\langle 00|\hat{Z}_2\hat{Z}_3|00\rangle_{2,3} = -\sin^2(\sqrt{2}Jt)$, whose modulus is 1 at $t = \pi/(2\sqrt{2}J)$. We have thus obtained a unit information flux (*i.e.* perfect state transfer) at the time predicted by the standard approach. Our simple example shows the basic features of IFA *at work*.

III. THE PROTOCOLS

A. Perfect state transfer

In order to properly understand our scheme for perfect state transfer, it is useful to consider the Hamiltonian

$$\hat{\mathcal{H}}_C = \sum_{i=1}^{N-1} J_i \hat{X}_i \hat{X}_{i+1} + \sum_{i=1}^{N} B_i \hat{Z}_i. \tag{2}$$

By analyzing the evolution of $\hat{X}_N$ and $\hat{Y}_N$ (in the Heisenberg picture) under the action of $\hat{\mathcal{H}}_C$, we obtain that $\hat{\tilde{X}}_N(t)$ and $\hat{\tilde{Y}}_N(t)$ can be written as

$$\begin{aligned}
\hat{\tilde{X}}_N(t) &= \mu_1(t)\hat{X}_N + \mu_2(t)\hat{Y}_N + \mu_3(t)\hat{X}_{N-1}\hat{Z}_N + \\
&+ \mu_4(t)\hat{Y}_{N-1}\hat{Z}_N + \cdots + \mu_{2N-1}(t)\hat{X}_1\hat{Z}_2\cdots\hat{Z}_N + \\
&+ \mu_{2N}(t)\hat{Y}_1\hat{Z}_2\cdots\hat{Z}_N, \\
\hat{\tilde{Y}}_N(t) &= \nu_1(t)\hat{X}_N + \nu_2(t)\hat{Y}_N + \nu_3(t)\hat{X}_{N-1}\hat{Z}_N + \\
&+ \nu_4(t)\hat{Y}_{N-1}\hat{Z}_N + \cdots + \nu_{2N-1}(t)\hat{X}_1\hat{Z}_2\cdots\hat{Z}_N + \\
&+ \nu_{2N}(t)\hat{Y}_1\hat{Z}_2\cdots\hat{Z}_N.
\end{aligned} \tag{3}$$

The time-dependent coefficients $\mu_i(t)$ and $\nu_i(t)$ are functions of J_i and B_i. Their explicit form is too cumbersome to be presented here. However, one can give a graphical picture of the way the operators entering Eqs. (3) are inter-related in terms of oriented graphs, as done in Ref. [23]. In particular, it is easy to check that such graphs are linear, in our case. An example, for $N = 3$, is given in Fig. 1 **(a)**. By explicitly analyzing $\mu_i(t)$ and $\nu_i(t)$, one recognizes that the information flux between $\hat{Y}_1$ ($\hat{X}_1$) and $\hat{X}_N$ ($\hat{Y}_N$) follows the same behavior as the

information flux $\hat{X}_1 \rightarrow \hat{X}_{2N}$ ($\hat{Y}_1 \rightarrow \hat{Y}_{2N}$) in an open $2N$-qubit chain ruled by

$$\hat{\mathcal{H}}_{eq} = \sum_{j=1}^{2N-1} J_j^{eq}(\hat{X}_j\hat{X}_{j+1} + \hat{Y}_j\hat{Y}_{j+1}) \qquad (4)$$

with $J_j^{eq} = B_{\frac{j+1}{2}}$ ($J_j^{eq} = J_{j/2}$) for odd (even) j. It is well known that perfect state transfer is achievable in a spin chain governed by the Hamiltonian in Eq. (4). In particular, if the parameters in Eq. (2) follow the pattern $J_i = \pm J\sqrt{4i(N-i)}$ (the choice of the signs needs to be consistent throughout the chain) and $B_i = J\sqrt{(2i-1)(2N-2i+1)}$ [3] and the initial state of all the qubits but the first one is $|0\rangle$, a unit (in modulus) information flux from $\hat{Y}_1$ ($\hat{X}_1$) to $\hat{X}_N$ ($\hat{Y}_N$) is found at the rescaled dimensionless time $Jt = \pi/4$. The information fluxes $\hat{Y}_1 \rightarrow \hat{X}_N$ and $\hat{X}_1 \rightarrow \hat{Y}_N$, for $N = 3$, are shown in Figs. 1 **(b)** and 1 **(c)**, respectively. This suggests that, by simply applying a single-qubit operator on the first spin before the evolution under the action of $\hat{\mathcal{H}}_C$ in Eq. (2) (the single-qubit operation being required in order to rotate the operator-basis of the first qubit and obtain unit flux between homonymous operators), perfect state transfer can be obtained. Under this point of view, our approach is quite non-conventional. In fact, instead of using a formal map between models (2) and (4), we gather our analytic results and design the optimal protocol in virtue of a quantitative analogy between the evolution of specific sets of operators as driven by the two interaction Hamiltonians we consider. We remark that this is possible solely because of the power of IFA. Hamiltonian (2) can be easily mapped onto the one

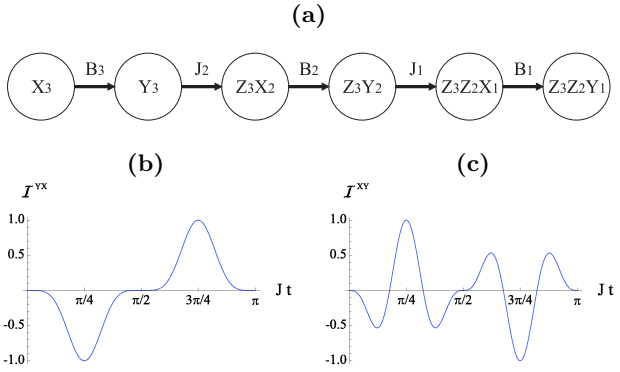

FIG. 1: **(a)**: Oriented graph describing the way the operators entering Eqs. (3) are related. The operator in each circle (a node) gives rise to its nearest neighbors under commutation with $\hat{\mathcal{H}}_C$ in Eq. (2), for $N = 3$. The oriented edges connect such nodes. The corresponding coefficients are also shown and an outgoing (ingoing) edge with respect to a node implies a $+$ ($-$) sign. **(b)**: Information flux from $\hat{Y}_1$ to $\hat{X}_N$ against the dimensionless interaction time Jt, for $N = 3$ and $J_i = \pm J\sqrt{4i(N-i)}$, $B_i = J\sqrt{(2i-1)(2N-2i+1)}$ in Eq. (2). Qubits 2 and 3 are prepared in $|00\rangle_{23}$. **(c)**: Information flux from $\hat{X}_1$ to $\hat{Y}_N$, for the same conditions as in panel **(b)**.

in Eq. (1) and perfect state transfer thus achieved with a further change of basis for all the qubits in the chain that transforms $|0\rangle_i \rightarrow |+\rangle_i$. Let us go into the details of the protocol. We prepare the first qubit in the state $|\psi\rangle_1 = \alpha|0\rangle_1 + \beta|1\rangle_1$ and apply the following recipe for perfect state-transfer:

- First step: The operator $T_1 \otimes H_1 \otimes T_1$ is applied to the first qubit of the chain, where $T_1 = |0\rangle_1\langle 0| + e^{i\frac{\pi}{2}}|1\rangle_1\langle 1|$ and $H_1 = (\sigma_x + \sigma_z)/\sqrt{2}$ is a Hadamard gate [24].
- Second step: The chain evolves under the action of $\hat{\mathcal{H}}$ for a time $Jt = \pi/4$.

In this way, the state of the last qubit will be $|\psi\rangle_N$, while the rest of the chain in the tensorial product state $|++..+\rangle_{1..N-1}$, thus achieving perfect state transfer.

The first step is required to cope with both the necessary basis changes (the first one to map the Hamiltonian $\hat{\mathcal{H}}$ onto $\hat{\mathcal{H}}_C$ and the second one to obtain unit fluxes between homonymous operators) and can be performed off-line. This corresponds to carrying out only the second step but using the initial state $|\tilde{\psi}\rangle_1 = [(\alpha + i\beta)|0\rangle_1 + (\beta + i\alpha)|1\rangle_1]/\sqrt{2}$. Alternatively, the change of basis can also be performed off-line at the end of the evolution driven by $\hat{\mathcal{H}}$. The initialization of the register in the tensorial product of $|+\rangle_i$ states can be obtained by cooling a thermal state of the qubit system to their own $|0\rangle_i$ state (thus achieving $|00\cdot\cdot0\rangle_{1..N}$, which is the standard initial state in quantum state-transfer protocols [3, 5]) and then applying single-qubit Hadamard gates. The same task can also be achieved by using a collective external potential resonant with the transition between the single-qubit levels, waiting enough time for the system to relax to the ground state and then applying the Hadamard gates.

B. Generation of multipartite entanglement

Interesting features arise from a deeper analysis of the model encompassed by $\hat{\mathcal{H}}$. Indeed, the same parameter pattern addressed up until now can be used so as to generate an N-qubit GHZ state $|GHZ\rangle_{12..N} = (\bigotimes_{i=1}^N |0\rangle_i - i\bigotimes_{i=1}^N |1\rangle_i)/\sqrt{2}$. If the initial state of every qubit is set to be $|0\rangle$, after the action of $\hat{\mathcal{H}}$ for a time $Jt = \pi/4$, the system will be in state $|GHZ\rangle_{12..N}$. This is understood by considering the fact that the evolution $e^{-i\frac{\pi}{4J}\hat{\mathcal{H}}}$ can be decomposed into the equivalent quantum circuit shown in Fig. 2 [11]. It is then straightforward to check that a GHZ state of the above mentioned form is the result of the computation described there.

It is very important to stress that our scheme to generate entanglement does not require any pre-built entanglement resource. Multipartite entanglement is generated in the chain only as a result of spin-non-preserving dynamics. An analogous situation has recently been addressed in [25].

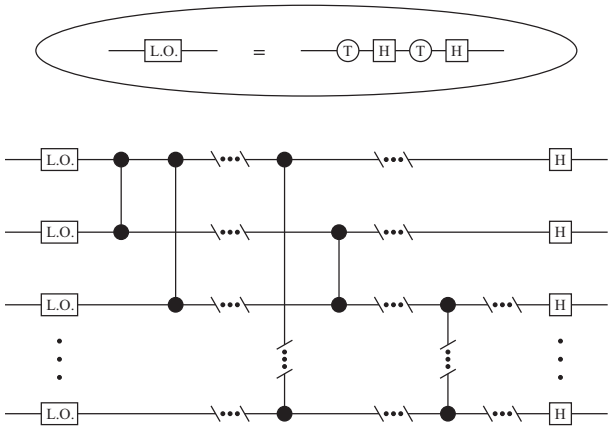

FIG. 2: Equivalent quantum circuit for a spin-chain that evolves according to $e^{-i\hat{\mathcal{H}}\frac{\pi}{4J}}$. The inset shows the explicit composition of the local operators before the inter-qubit interaction structure. We show the symbols for T, H and controlled-phase operations. For clarity of presentation, we have omitted to show a set of swap gates (performing mirror-inversion) at the end of the circuit.

IV. EFFECTS OF STATIC DISORDER, DECAY AND DECOHERENCE

We address the effects of static disorder in the pattern of coupling strengths which is required for the optimal performance of the protocols. This is useful in a general situation, and particularly necessary in the case of superconducting qubits. Although control over lithographic techniques being used in the fabrication of superconducting qubits is constantly being improved, it is reasonable to expect that the elements of a long chain of effective spins would not be identical and the inter-qubit couplings will correspondingly be affected. We also consider the influences of Markovian dissipation and phase-decoherence on the state transfer and the creation of a multipartite GHZ state. In order to account for the usual finite spatial environmental correlation length that frequently affects solid-state systems, we address both the case of uncorrelated individual baths being coupled to the spins in a chain as well as the case of the same bosonic environment affecting multiple spins simultaneously. Our study reveals not only a considerable resilience of the protocols at hand but also points out some interesting features that highlight the counter-intuitive nature of noise effects in purely quantum dynamics. It is worth stressing that, as we study a coupling model with a novel pattern of interaction strengths, which is different from the one given in [3], an investigation about noise effects is quite significant and represents a due step in the full characterization of the scheme we study. Such a program is in line with previous studies on fluctuation and noise in state transfer protocols, which can be found in Refs. [26, 27].

A. Perfect state transfer

We start by analyzing the effects of static disorder in the coupling-strength pattern for the state transfer protocol. Our model for such imperfections is that of a distribution of coupling strengths along the chain according to [26]

$$\begin{aligned} J_i \to \mathcal{J}_i &= J_i[1+\delta(1-2r_i)], \\ B_i \to \mathcal{B}_i &= B_i[1+\delta(1-2s_i)] \end{aligned} \tag{5}$$

with δ the 'strength' of the disorder (typically a few percent of J) and $r_i, s_i \in [0,1]$ that decide whether the imperfect parameter is larger or smaller than the ideal value. In our study, we take r_i's and s_i's as random numbers following a given probability distribution. Clearly, the choice of such a distribution should be made consistent with a given experimental situation. Here, in order to gather a simple idea of what the effect of static disorder is, a uniform distribution is chosen. Intuitively, this case should depict a sort of 'worst case' scenario for the influences of disorder. We show that, for values of δ which are within the current accuracy of lithographic fabrication of superconducting qubits, this class of imperfections does not significantly affect the performance of quantum state transfer in our chain.

The figure of merit that we choose in order to test the performance of the protocol affected by disorder is the state fidelity between the logical input qubit and the state of the N^{th} physical qubit of the chain at time $t = \pi/4J$. Indeed, while it is reasonable to expect that disorder would influence the state of the rest of the chain, leaving it in a state different from the expected $\bigotimes_{i=1}^{N-1}|+\rangle_i$, this is irrelevant in a state-transfer problem. Clearly, in a real physical situation, we have no available information on the exact value of the disordered coupling strengths' pattern. This implies that a faithful measure of the quality of our protocol would be rather given by the average of state fidelity over a large sample of disorder configurations (from now on called *runs*). That is, if we indicate as $\mathcal{F}_{1N}(\delta,\{r_i,s_i\}_k) = \langle ist|\varrho_N^{\delta,\{r_i,s_i\}_k}|ist\rangle$ the state fidelity corresponding to a given run labelled by the integer $k = 1, 2, .., M$ (with $|ist\rangle$ is the ideal state to transfer and $\varrho_N^{\delta,\{r_i,s_i\}_k}$ the reduced density matrix of the last qubit of the chain), we will consider the average value

$$\mathcal{F}_{1N}^{av} = \frac{1}{M}\sum_{k=1}^{M}\mathcal{F}_{1N}(\delta,\{r_i,s_i\}_k). \tag{6}$$

The cut-off M in the estimation of the average is taken large enough to guarantee that no appreciable differences in $\mathcal{F}_{1N}^{av}$ are observed if a larger M is taken.

We first consider a state-dependent situation based on an analogy with existing studies on quantum state transfer. We will shortly demonstrate that the state fidelity of the process is very weakly dependent on the input state being considered. However, in order to fix

the ideas, we consider the arbitrarily chosen input state $|-\rangle_1 = (|0\rangle_1 - |1\rangle_1)/\sqrt{2}$. As a trade off between required computational power and length of the chain, we have examined the case of $N = 7$ qubits throughout the paper (where not stated differently). Although the results presented in our study depend on the length of the chain system being studied, we have checked that such a dependence is very weak and our findings can be taken as faithful indications of the behavior of even longer chains. As the maximum of fidelity is expected for $Jt = \pi/4$, we restrict our observation to a temporal window centered in this value. In Fig. 3, we compare the ideal and the disordered situation for a strength $\delta/J = 5\%$, which is a typical in state of the art value [28].

Evidently, the influence of disorder is negligible, at least for the operating conditions considered above: not only is the height of the fidelity peak preserved almost perfectly, but also such peak occurs precisely at the rescaled time that is expected under ideal performances. This is important, experimentally, as it proves that our state of ignorance over the exact value of the disordered coupling strengths does not require the fine adjustment of the time at which the logical qubit to be transferred should be collected.

As a step forward in the analysis of the protocol, we now remove any dependence on the logical state to be transferred. We take a 'black box' perspective under which the problem at hand is not different from that of characterizing an unknown operation (the transfer channel with disorder) with respect to an ideal one which would map the logical input state onto the same state at the N^{th} physical qubit, leaving the logical input state unchanged. Such a characterization is efficiently performed by using quantum process tomography (QPT) techniques [29, 31], which has proven to be invaluably useful in many experimental contexts [30]. QPT is a useful tools for the evaluation of the global closeness between the ideal and disordered transfer channel. By studying the way the black box affects the transfer of the four *probe states* $\{|0\rangle, |1\rangle, |+\rangle, |+_y\rangle\}$, we can reconstruct the so-called *process matrix* χ_{dis} of the disordered process. This contains all the relevant information regarding the process that a logical qubit undergoes in being transferred from the first to the last physical qubit. We refer

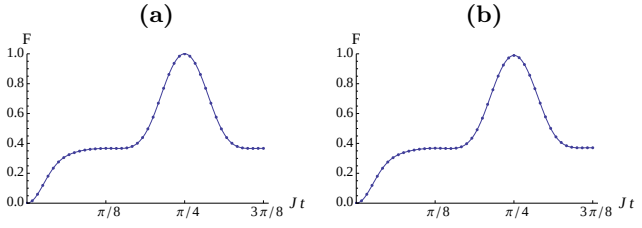

FIG. 3: **(a)**: State fidelity against dimensionless time Jt with no disorder and $N = 7$; **(b)**: Same with $\delta = 0.05$, corresponding to a 5% maximum deviation of the disordered parameters from the ideal values.

to existing literature [29, 31] for further mathematical details and just mention that the QPT approach can also be computationally beneficial as the averaged state fidelity can be calculated out of the process fidelity

$$F_p = \mathrm{Tr}(\chi_{id}\chi_{dis}) \tag{7}$$

with χ_{id} the process matrix of the logical identity operation that is applied to the logical qubit to transfer in the perfect case. In the operator basis $\{\hat{\mathbb{1}}, \hat{X}, -i\hat{Y}, \hat{Z}\}$, this reads

$$\chi_{id} = \begin{pmatrix} 1 & 0 & 0 & 0 \\ 0 & 0 & 0 & 0 \\ 0 & 0 & 0 & 0 \\ 0 & 0 & 0 & 0 \end{pmatrix}. \tag{8}$$

QPT allows the reconstruction of the effective Kraus operators of the disordered transfer channel and, from these, one can easily get the output density matrix for any logical input state. In turn, by using the correspondence between density matrix and Bloch vector, we can visualize the effect of the disorder directly on the Bloch sphere of the transferred state, thus getting a general overview of the behavior of the protocol. Given the results in Fig. 3, the output Bloch sphere with disorder strength $\delta/J = 5\%$ at $Jt = \pi/4$ should be very close to the Bloch sphere of a pure qubit state. This is indeed the case, as shown in Fig. 4, where panel **(a)** shows the Bloch sphere for the ideal protocol, while panel **(b)** addresses the case of the disordered pattern corresponding to the worst fidelity among 200 runs. The two processes are evidently quite close to each other, the most evident difference being a slight unwanted rotation of the sphere's poles around the x axis. We have checked that the rotation angle is an increasing function of the disorder's strength. No shrinking of the sphere for the disordered case is evident, showing that coherence and amplitude of the logical qubit are almost perfectly preserved. The matrix of the disordered process is given by

$$\chi_{dis} = \begin{pmatrix} 0.987 & 0.003 + 0.022i & 0 & 0 \\ 0.003 - 0.022i & 0.001 & 0 & 0 \\ 0 & 0 & 0.008 & 0.003 \\ 0 & 0 & 0.003 & 0.005 \end{pmatrix}, \tag{9}$$

which corresponds to a state fidelity of 0.991. The state fidelity averaged over the whole set of runs is as large as 0.995. The closeness of this number to the worst-case fidelity shows that the disordered state transfer process depends only very weakly on the pattern of disorder. On the other hand, the evident isotropy of the reconstructed Bloch sphere justifies an arbitrary choice of the input state for our explicit analysis. We can therefore confidently affirm that, within the range of chain's length we have studied, static disorder does not spoil the process we have designed for perfect state transfer across a chain. The average fidelity of the process stays largely above 2/3, the highest value for a classical transmission of a state [32], up until values of $\delta/J \sim 30\%$.

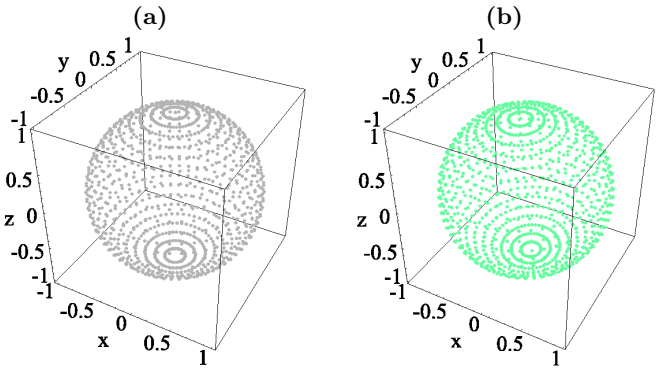

FIG. 4: **(a)**: Bloch sphere of the logical input qubit for various choices of α. **(b)**: Reconstructed Bloch sphere showing the state of the N^{th} qubit for a disordered chain of $N = 7$ and $\delta/J = 5\%$ at $Jt = \pi/4$.

.

We now consider the effects of dissipation and decoherence on the protocol. We assume conditions of weak coupling of the spins of the chain with the environment, so that a spin-boson approach can be retained and the consequent non-unitary dynamics can be studied within the context of a Lindbladian approach or, equivalently, an operator-sum representation of the evolution [33]. By choosing this second perspective, as it will clearly appear in what follows, we model our study along the lines of a Monte Carlo simulation. The environmental action over the chain is identified in the effects of both amplitude and phase damping channels. First, we address the case of N individual baths, one for each spin of the chain. This assumption is physically motivated by considering that each Josephson charge qubit has its own voltage gate and can thus suffer *individual* electromagnetic fluctuations. Then in order to account for the finite spatial correlation length of a Markovian environment, which may occur in solid-state systems, we consider a bosonic environment affecting more than a single spin simultaneously (as can be the case for a bath of background phonons arising from the common substrate onto which the charge qubits are placed). In the following, we show a considerable robustness of the state transfer protocol against both these sources of imperfection and the appearance of some counter-intuitive features that can be related to the phenomenon of stochastic resonances [12].

In an operator-sum representation, the evolution of an initial state ϱ_c of the whole chain under the effect of an environment is given by

$$\varrho_c(t) = \sum_{\mu} \hat{K}^{\mu}(t)\varrho_c\hat{K}^{\mu\dagger}(t) \tag{10}$$

with $\{\hat{K}^{\mu}(t)\}$ a set of time-dependent Kraus operators, having the structure of a tensorial product of single-spin operators and such that $\sum_{\mu}\hat{K}^{\mu\dagger}(t)\hat{K}^{\mu}(t) = \mathbb{1}$ [24, 33]. The formal description of a single-spin amplitude damping process in a bath at finite temperature is described by the trace-preserving completely positive map given by the following set of Kraus operators [24]:

$$\hat{A}_i^0 = \sqrt{p}\begin{pmatrix}1 & 0\\ 0 & e^{-\frac{\Gamma t}{2}}\end{pmatrix},\ \hat{A}_i^1 = \sqrt{p}\begin{pmatrix}0 & \sqrt{1-e^{-\Gamma t}}\\ 0 & 0\end{pmatrix}$$
$$\hat{A}_i^2 = \sqrt{1-p}\begin{pmatrix}e^{-\frac{\Gamma t}{2}} & 0\\ 0 & 1\end{pmatrix},\ \hat{A}_i^3 = \sqrt{1-p}\begin{pmatrix}0 & 0\\ \sqrt{1-e^{-\Gamma t}} & 0\end{pmatrix} \tag{11}$$

with $p = (\overline{n}+1)/(2\overline{n}+1)$ and $\overline{n}$ the average phonon number of each bath. For a phase damping channel, on the other hand, we have the following set [24]

$$\hat{D}_i^0 = \sqrt{\frac{1+e^{-\gamma t}}{2}}\hat{\mathbb{1}}_i,\ \hat{D}_i^1 = \sqrt{\frac{1-e^{-\gamma t}}{2}}\hat{Z}_i. \tag{12}$$

In the above equations, Γ and γ are the rates of amplitude and phase damping, respectively. On the other hand, clearly, the unitary dynamics determined by the coupling Hamiltonian in Eq. (2) leads to $\varrho_c(t) = e^{-i\hat{\mathcal{H}}t}\varrho_c e^{i\hat{\mathcal{H}}t}$. Our approach is to intersperse a unitary evolution lasting for a time interval Δt with non-unitary dynamics. Δt is taken randomly according to the general recipe for Quantum Monte Carlo simulations (see Ref. [34], for instance). Moreover, we randomly determine the set of Kraus operator to apply and the specific spin being affected. The disorder's pattern is kept as fixed for the duration of one of such simulated dynamics. In virtue of the weak dependence of state fidelity on δ, a random choice of the disorder configuration will be enough. The state fidelity resulting from the simulated dynamics has then to be averaged over a collection of noise-occurrence patterns (runs), which guarantees the faithful unraveling of the open quantum dynamics [34]. For our numerical study, whose results are presented in Fig. 5 **(a)**, we have taken the input state $|-\rangle_1$ with $\delta/J = 5\%$, $\gamma/J = 0.5$, $\Gamma/J = 0.2$ and $\overline{n} = 0.01$ in a chain of 7 qubits and a sample of 200 runs [35]. Evidently, the state fidelity is close to 0.95, which is an excellent result. Again, the peak of fidelity is obtained at the expected value $Jt = \pi/4$, although the effects of noise and decoherence, altering the pattern of quantum interference that is at the basis of a state transfer process [5, 6], could

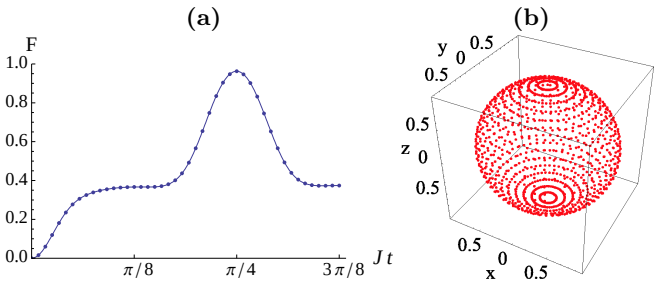

FIG. 5: **(a)**: Fidelity $\mathcal{F}_{1N}^{av}$ for an input state $|-\rangle_1$ against Jt with $\delta/J = 5\%$, $\Gamma/J = 0.5$, $\gamma/J = 0.2$, $\overline{n} = 0.01$ and $N = 7$. The average fidelity is calculated over a set of 200 disordered patterns. **(b)**: Bloch sphere of the output qubit evaluated with QPT for the same parameters assumed in panel **(a)**.

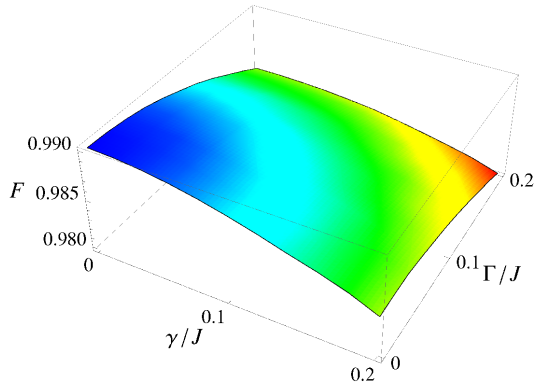

FIG. 6: Fidelity $\mathcal{F}_{1N}^{av}$ versus γ/J and Γ/J for $Jt = \pi/4$, $\delta/J = 5\%$, $\overline{n} = 0.01$ and $N = 6$.

also have resulted in a shift of the peak. A more complete picture comes from the analysis by means of QTP. As before, we have chosen a random configuration of disordered coupling strengths and have then evaluated the effects of decoherence and dissipation on a generic input state, obtaining the output Bloch sphere in Fig. 5 **(b)**. The effects of noise seem to result in just a small uniform shrinking of the Bloch sphere. The average fidelity of the process is 0.959.

In order to evaluate the relative *weight* of the two noisy channels over the state fidelity, we have plotted its maximum against γ and Γ and for one randomly generated disorder pattern (Fig. 6). In this case, we needed to reduce the number of qubits in the chain to $N = 6$ and increase the number of runs to obtain a better plot. Moreover, in order to exclude any dependence on the input state, we have averaged the state fidelity over a large sample of random pure input states. In virtue of the almost perfect insensitivity of the protocol to the specific instance of input state, this step turned out to be rather conservative. The most relevant feature appearing from this study is that, for a fixed value of γ, the state fidelity has a (weak) non-monotonic convex behavior against Γ. As this feature is not well visible from Fig. 6, we have considered a bidimensional projection of this plot along the cut $\gamma = 0.2J$ in Fig. 7, where the interaction time is fixed at $Jt = \pi/4$. The existence of a small peak of fidelity for increasing value of the dissipation rate can be interpreted following the lines of Ref. [12], where the phenomenon of *quantum stochastic resonances* has been extended to a multiparticle setting and invoked as the mechanism behind counter-intuitive features of benchmarks such as entanglement against the influences of noise [12, 36]. We observe that a *not too weak* dissipative mechanism alters the occurrence of quantum interference so as to improve the performances of the state transfer protocol. This effect obviously disappears as soon as the dissipation is so strong for the system to cope with it in a coherent way. The non-monotonic transmission fidelity provides us with a new way to characterize the response of a system which differs from the figures of merit used in [12], where dynamical properties (such as the chain's magnetization) or information theoretic ones (such as the mutual information) have been used as a measure of global correlations. Our study goes along the lines of previous results by Mancini and Bowen [37], where the rate of transmission of information through a class of quantum channels is shown to increase with the external noise. The results of our investigation motivate further studies of stochastic resonance phenomena in the context of information transmission through quantum channels.

We conclude our analysis of the effects of realistic imperfections on the proposed protocol for quantum state transfer by addressing the case of baths having a longer correlation length, so as to give rise to non-localized environmental effects. The analysis so far has been done by considering every qubit interacting with its own independent bath. As explained before, the substrate where our hypothetical superconducting chain is fabricated could provide a mechanism for correlated noise at longer haul. In this case the qubits can be considered, in first instance, to interact with shared baths. Here, in order to provide an intuitive idea of the general behavior of the protocol with respect to this situation, we consider the simplest case in which we have a collection of independent baths, each affecting a pair of spins at the same time. In order to model the evolution of the system in this scenario we use the operator-sum representation corresponding to the set of Kraus operators for two-qubit collective phase

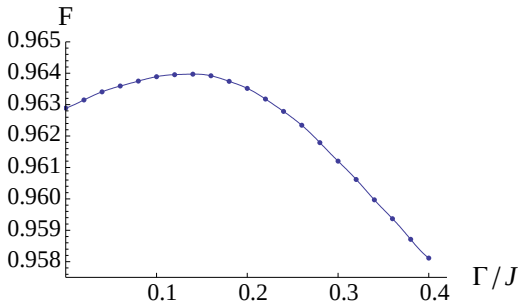

FIG. 7: Fidelity $\mathcal{F}_{1N}^{av}$ with $N = 6$ at $Jt = \pi/4$, $\delta/J = 5\%$, $\gamma/J = 0.2$, $\overline{n} = 0.01$ against Γ/J. The transmission fidelity is maximal for an optimal value of the environmental noise and is the result of the average over many noisy and disordered runs. The fact that the efficiency of the protocol depends non-monotonically on the noise strength can be viewed as a form of stochastic resonance.

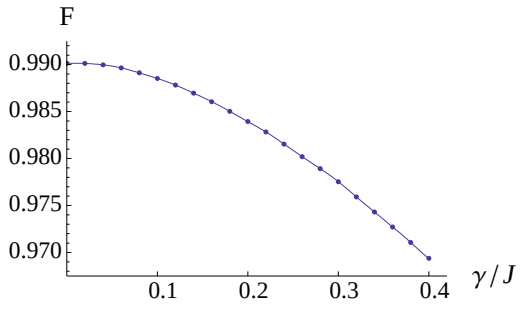

FIG. 8: Fidelity $\mathcal{F}_{1N}^{av}$ for a chain interacting with collective baths addressing two qubits simultaneously with $Jt = \pi/4$, $\delta/J = 5\%$ and $N = 6$ against γ/J and in absence of dissipation.

damping noise (see Ref. [38], for instance)

$$\hat{D}_0^c = \begin{pmatrix} e^{-\gamma t/2} & 0 & 0 & 0 \\ 0 & 1 & 0 & 0 \\ 0 & 0 & 1 & 0 \\ 0 & 0 & 0 & e^{-\gamma t/2} \end{pmatrix},$$

$$\hat{D}_1^c = \sqrt{1-e^{-\gamma t}} \begin{pmatrix} 1 & 0 & 0 & 0 \\ 0 & 0 & 0 & 0 \\ 0 & 0 & 0 & 0 \\ 0 & 0 & 0 & -e^{-\gamma t} \end{pmatrix}, \qquad (13)$$

$$\hat{D}_2^c = (1-e^{-\gamma t}) \begin{pmatrix} 0 & 0 & 0 & 0 \\ 0 & 0 & 0 & 0 \\ 0 & 0 & 0 & 0 \\ 0 & 0 & 0 & \sqrt{1+e^{-\gamma t}} \end{pmatrix}.$$

Due to our choice of two qubit-addressing collective bath, here we consider a chain of six qubits. Clearly, the analysis can be extended to any number of qubits being simultaneously addressed. We have obtained the plot in Fig. 8. In the presence of phase decoherence alone, no stochastic resonance effects are observable. The fidelity decreases monotonically as a function of γ/J, which agrees with all previous literature [39], where the emergence of stochastic resonance phenomena was shown to require the presence of noise forms that couple transversely to the localized basis states.

Although the Hamiltonian model we have considered does not enjoy particularly symmetries with respect to the coupling with the collective baths, so that no genuine phase-damping decoherence free subspace can be singled out, the resilience of the protocol is evident. The results are comparable to the case of individual environment attached to each spin and we have checked that this feature does not depend on the number of qubits being affected at the same time by a given bath [40].

B. Generation of multipartite entanglement

We now pass to a brief analysis of the proposed protocol for GHZ-state generation along the lines described in the previous part of our study. However, here there is an important technical difference that has to be stressed: differently from what has been done above, here we need to consider the global fidelity of chain with a GHZ state of the form $|GHZ\rangle_{12..N} = (\bigotimes_{i=1}^{N} |0\rangle_i - i \bigotimes_{i=1}^{N} |1\rangle_i)/\sqrt{2}$. Indeed, we are now interested in the generation of a multipartite entangled state where every qubit will be involved. We have evaluated the evolution of the system in the noisy scenario. We take advantage of the analysis performed in the previous Section and in order to avoid unnecessary redundancy, we present here the results obtained including static disorder, dissipation and phase decoherence, without considering them individually.

Fig. 9 shows the fidelity against dimensionless time Jt in the ideal case [panel **(a)**] and for the same values of disorder, decoherence and dissipation rates and temperature used previously [panel **(b)**]. The chain we have considered is seven-qubit long and the state fidelity has been averaged over 200 different runs. Although the performance of the protocol seems to be inferior to the one corresponding to quantum state transfer, we should keep in mind that here we are using a global figure of merit. Moreover, despite the fragility of GHZ-like entanglement to various forms of noisy channels [41], the resilience of the imperfect multipartite-entanglement generation protocol is still quite satisfactory (maximum fidelity larger than 0.88).

V. CONCLUDING REMARKS

We have used information flux methods in order to design a protocol for quantum state transfer in a finite, open chain of qubits. The protocol is based on a nontrivial map between the algebra of angular momenta an a control-limited Ising-like Hamiltonian with additional local magnetic fields. The dynamics described by such a coupling is rich enough to provide an effective way of performing a multipartite entangling gate among the elements of the register, which produces GHZ-like entanglement. Both these protocols have been analyzed in terms of their resilience against certain realistic sources of disorder and decoherence and were found to be rather robust. Moreover, our study has uncovered an unexpected relation between state-transfer fidelity and quan-

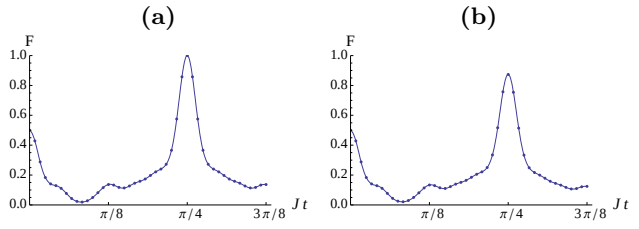

FIG. 9: **(a)**: State fidelity for GHZ-state generation against dimensionless time Jt in the ideal case and $N = 7$; **(b)**: Same with disorder $\delta/J = 5\%$, $\gamma/J = 0.5$, $\Gamma/J = 0.2$ and $\overline{n} = 0.01$.

tum stochastic resonances, thus giving our pragmatically-oriented work a more fundamental character. Our investigation contributes to the affirmation of information flux-based methods in the design of multipartite systems in control-limited scenarios and to the ubiquitous nature of stochastic resonance mechanisms, two points which certainly deserve further studies.

Acknowledgments

We thank F. Ciccarello, M. S. Kim, M. B. Plenio, and M. S. Tame for fruitful discussions. We acknowledge support from the EPSRC, the QIPIRC, and the FP6-IP QAP ("Qubit Applications"). M.P. was supported by The Leverhulme Trust (Grant No. ECF/40157) and the Bridging Fund from Queen's University Belfast. D.I.T. was supported by EPSRC (EP/D065305/1).

[1] L. Amico, R. Fazio, A. Osterloh, and V. Vedral, Rev. Mod. Phys, **80**, 517 (2008), and references within.
[2] S. C. Benjamin and S. Bose, Phys. Rev. Lett. **90**, 247901 (2003).
[3] M. Christandl, N. Datta, A. Ekert, and A. J. Landahl, Phys. Rev. Lett. **92**, 187902 (2004); C. Albanese, M. Christandl, N. Datta, and A. Ekert, Phys. Rev. Lett. **93**, 230502 (2004); M. Christandl, N. Datta, T. C. Dorlas, A. Ekert, A. Kay, and A. J. Landahl, Phys. Rev. A **71**, 032312 (2005).
[4] P. Kok, W. J. Munro, K. Nemoto, T. C. Ralph, J. P. Dowling, and G. J. Milburn, Rev. Mod. Phys. **79**, 135 (2007).
[5] S. Bose, Phys. Rev. Lett. **91**, 207901 (2003).
[6] M. B. Plenio, J. Hartley and J. Eisert, New J. Phys., **6**, 36 (2004); M. Paternostro, G. M. Palma, M. S. Kim, and G. Falci, Phys. Rev. A **71**, 042311 (2005); D. Burgarth, and S. Bose, Phys. Rev. A **71**, 052315 (2005); V. Giovannetti, and D. Burgarth, Phys. Rev. Lett. 96, 030501 (2006); O. Romero-Isart, K. Eckert, and A. Sanpera, Phys. Rev. A **75**, 050303(R) (2007); A. Kay, Phys. Rev. Lett. **98**, 010501 (2007); A. Biswas, and G. S. Agarwal, Phys. Rev. A **70**, 022323 (2004); M. B. Plenio, and F. L. Semiao, New J. Phys. **7**, 73 (2005).
[7] R. Horodecki, P. Horodecki, M. Horodecki, K. Horodecki, e-print arXiv:quant-ph/0702225 (2007); M. B. Plenio and S. Virmani, Quant. Inf. Comp. **7**, 1 (2007).
[8] D. M. Greenberger, M. A. Horne and A. Zeilinger, *Bell Theorem, Quantum Theory, and Conceptions of the Universe* Ed M. Kafatos (1989 Dordrecht: Kluwer) pag. 69.
[9] M. Hillery, V. Bužek, and A. Berthiaume, Phys. Rev. A **59**, 1829 (1999); C. Schmid, P. Trojek, M. Bourennane, C.Kurtsiefer, M. Zukowski, and H. Weinfurter, Phys. Rev. Lett. **95**, 230505 (2005).
[10] A. M. Wang, Phys. Rev. A **75**, 062323 (2007); C. Di Franco, M. Paternostro, and M. S. Kim, Phys. Rev. A **75**, 052316 (2007); M. Christandl and S. Wehner, in *Proceedings of 11th International Conference on the Theory and Application of Cryptology and Information Security (ASIACRYPT 2005)*, Lecture Notes in Computer Science Vol. 3788 (Springer, Berlin, 2005), p. 217.
[11] For an analogous decomposition performed with respect to Eq. (4), see S. R. Clark, C. Moura Alves, and D. Jaksch, New J. Phys. **7**, 124 (2005).
[12] M. B. Plenio and S. F. Huelga, Phys. Rev. Lett. **88**, 197901 (2002); S. F. Huelga and M. B. Plenio, Phys. Rev. Lett. **98**, 170601 (2007).
[13] Y. Makhlin, G. Schön, Schnirman, Rev. Mod. Phys. **73**, 357 (2001).
[14] J. Q. You and F. Nori, Phys. Today **58**, 42 (2005).
[15] D. I. Tsomokos, M. J. Hartmann, S. F. Huelga, and M. B. Plenio, New J. Phys. **9**, 79 (2007).
[16] D. Vion, A. Aassime, A. Cottet, P. Joyez, H. Pothier, C. Urbina, D. Esteve, and M. H. Devoret, Science **296**, 886 (2002).
[17] Y. A. Pashkin, T. Yamamoto, O. Astafiev, Y. Nakamura, D. V. Averin, J. S. Tsai, Nature (London) **421**, 823 (2003); T. Yamamoto, Y. A. Pashkin, O. Astaviev, Y. Nakamura, J. S. Tsai, Nature (London) **425**, 941 (2003).
[18] J. Plantenberg, P. C. de Groot, C. J. P. M. Harmans, J. E. Mooij, Nature (London) **447**, 836 (2007).
[19] For a recent account of experiments with superconducting qubits that are coupled in a controllable way, see S. Ashhab, A. O. Niskanen, K. Harrabi, Y. Nakamura, T. Picot, P. C. de Groot, C. J. P. M. Harmans, J. E. Mooij, F. Nori, e-print arXiv:0709.0237 (2007).
[20] J. E. Mooij, private communication.
[21] E. Lieb, T. Schultz, and D. Mattis, Ann. Phys. **16**, 407 (1961); S. Sachdev, *Quantum phase transitions* (Cambridge University Press, Cambridge, 1999).
[22] C. Di Franco, M. Paternostro, G. M. Palma, and M. S. Kim, Phys. Rev. A **76**, 042316 (2007).
[23] C. Di Franco, M. Paternostro, and G. M. Palma, e-print arXiv:0802.3980 (2008).
[24] M. A. Nielsen and I. L. Chuang, *Quantum Computation and Quantum Information* (Cambridge University Press, Cambridge, 2000).
[25] C. Di Franco, M. Paternostro, and M. S. Kim, Phys. Rev. A **77**, 020303(R) (2008).
[26] For a different model of disorder, see G. De Chiara, D. Rossini, S. Montangero, and R. Fazio, Phys. Rev. A **72**, 012323 (2005).
[27] D. Burgarth, Eur. Phys. J. Special Topics **151**, 147 (2007); M. Wiesniak, e-print arXiv:0711.2357 (2007), C. K. Burrell, and T. J. Osborne, Phys. Rev. Lett. **99**, 167201 (2007); L. Zhou, J. Lu, T. Shi, and C. P. Sun, e-print arXiv:0608135 (2006).
[28] For charge qubits at 20-40 mK the typical disorder strength is between 5 and 10% (Floor Paauw and Pieter de Groot, private communication).

[29] I. L. Chuang and M. A. Nielsen, J. Mod. Opt. **44**, 2455 (1997).

[30] M. A. Nielsen, E. Knill, and R. Laflamme, Nature (London) **396**, 52 (1998); J. B. Altepeter, D. Branning, E. Jeffrey, T. C. Wei, P. G. Kwiat, R. T. Thew, J. L. O'Brien, M. A. Nielsen, and A. G. White, Phys. Rev. Lett. **90**, 193601 (2003); J. L. O'Brien, G. J. Pryde, A. Gilchrist, D. F. V. James, N. K. Langford, T. C. Ralph, and A. G. White, Phys. Rev. Lett. **93**, 080502 (2004); N. K. Langford, T. J. Weinhold, R. Prevedel, A. Gilchrist, J. L. O'Brien, G. J. Pryde, and A. G. White, Phys. Rev. Lett. **95**, 210504 (2005); Y. Nambu and K. Nakamura, Phys. Rev. Lett. **94**, 010404 (2005); M. Howard, J. Twamley, C. Wittmann, T. Gaebel, F. Jelezko and J. Wrachtrup, New J. Phys. **8**, 33 (2006); T. Yamamoto, R. Nagase, J. Shimamura, S. K. Özdemir, M. Koashi, and N. Imoto, New J. Phys. **9**, 191 (2007); R. Prevedel, M. S. Tame, A. Stefanov, M. Paternostro, M. S. Kim, and A. Zeilinger, Phys. Rev. Lett. **99**, 250503 (2007).

[31] M. S. Tame, M. Paternostro, and M. S. Kim, New J. Phys. **9**, 201 (2007).

[32] M. Horodecki, P. Horodecki, and R. Horodecki, Phys. Rev. A **60**, 1888 (1999).

[33] J. Preskill, Lecture notes in physics, available at http://www.theory.caltech.edu/people/preskill/ph229/.

[34] J. Dalibard, Y. Castin, and K. Mølmer, Phys. Rev. Lett. **68**, 580 (1992); M. B. Plenio and P. L. Knight, Rev. Mod. Phys. **70**, 101 (1998).

[35] For weakly coupled spins $J \sim 1$GHz is experimentally reasonable in charge qubits (the coupling between two qubits in Ref. [17] was around 10GHz). This implies the rather pessimistic values of $\Gamma^{-1} \sim 0.2$ns and $\gamma^{-1} \sim 0.5$ns, which are one order of magnitude smaller than the decoherence time estimated experimentally in [17] for two coupled charge qubits.

[36] L. Hartmann, W. Dür and H.-J. Briegel, Phys. Rev. A. **74**, 052304 (2006); L. Hartmann, W. Dür, and H.-J. Briegel, New J. Phys. **9**, 230 (2007).

[37] G. Bowen and S. Mancini, Phys. Lett. A **352**, 272 (2006).

[38] T. Yu and J. H. Eberly, Opt. Commun. **264**, 393 (2006).

[39] D. E. Makarov and N. Makri, Phys. Rev. B **52**, R2257 (1995); M. Grifoni and P. Hänggi, Phys. Rev. Lett. **76**, 1611 (1996); S. F. Huelga and M. B. Plenio, Phys. Rev. A **62**, 052111 (2000); T. Wellens and A. Buchleitner, Phys. Rev. Lett. **84**, 5118 (2000); L. Viola, E. M. Fortunato, S. Lloyd, C.-H. Tseng, and D. G. Cory, Phys. Rev. Lett. **84**, 5466 (2000).

[40] As an additional remark, we briefly mention about the possibility of an error in the timing of the process. The protocol requires the extraction of the logical state after the precise time $t = \pi/(4J)$, which corresponds to the maximum of the state fidelity. This is obviously equivalent to switching off the mutual inter-spin interaction at time $\pi/(4J)$ and extracting the state at the N^{th} spin in the chain. As we have already said, a realistic choice for J is in the range of 1GHz (it can be larger) while the temporal window within which, typically, the state fidelity is larger than 0.9 (an arbitrary and rather conservative choice) is as large as $J\Delta t \simeq 0.2$. This leads to Δt being typically in the range of 0.1ns, which can be perfectly resolved experimentally [17].

[41] C. Simon and J. Kempe, Phys. Rev. A **65**, 052327 (2002); M. S. Tame, M. Paternostro, M. S. Kim, and V. Vedral, Int. J. Quant. Inf. **4**, 689 (2006).